Available online at www.sciencedirect.com
ScienceDirect
Nuclear Instruments and Methods in Physics Research A 566 (2006) 713–721
NUCLEAR INSTRUMENTS & METHODS IN PHYSICS RESEARCH Section A
www.elsevier.com/locate/nima

A wide-beam X-ray source suitable for diffraction enhanced imaging applications

Chang H. Kim*, Mohamed A. Bourham, J. Michael Doster

Department of Nuclear Engineering, North Carolina State University, Raleigh, NC 27695-7909, USA

Received 10 February 2006; received in revised form 5 July 2006; accepted 16 July 2006
Available online 11 August 2006

Abstract

Research in diffraction-enhanced imaging (DEI), using a synchrotron source with an X-ray flux of 1.4×10^{12} ph/mm^2/s, has shown strong potential in obtaining high-resolution images as compared to conventional radiographs. This research investigates the feasibility of developing a large area circular X-ray source with fluxes comparable to a synchrotron source. The source should be capable of integration into a compact system with peak powers not to exceed 200 kW to be feasible for use in a major medical facility, industrial complex or screening facility (such as cargo or airport). A computational study of a circular concentric filament wide-beam area X-ray source has been investigated in this research. The design features are based on generating electrons from three concentric circular filaments to provide an area electron flux, with a 60 kV accelerating potential and a beam current of up to 3 A. The X-ray target is a grounded stationary oxygen-free copper target with a layer of molybdenum. This target feature differs from standard rotating X-ray targets in conventional X-ray systems. Studies of electron trajectories and their distribution on the target were conducted using the SIMION 3D code. Heat loading and thermal management were studied using heat transfer modules from the coupled FEMLAB multi-physics and MATLAB codes. The Monte Carlo code MCNP 5 was used to obtain the X-ray flux and energy distribution for aluminum and beryllium windows. This computational study shows that this target configuration generates X-rays with photon flux comparable to synchrotron source and sufficient for DEI applications. The maximum target temperature rise is 1357 K after 70 s when cooling the back of the target to liquid nitrogen temperature using cold finger contact, and 325 K for an invaded target, in which liquid nitrogen circulates inside the target.

PACS: 41.50.+h; 41.85.Ew; 32.30.Rj; 87.59.−e

Keywords: Diffraction enhanced imaging; Electron trajectory; Heat conduction; Characteristic X-ray

1. Introduction

Although development of digital mammography has enabled better diagnosis with the integration of advanced image digital processing [1], images produced through diffraction-enhanced imaging techniques have proven to be of high quality as image scattering is eliminated [2–4]. In the preliminary work of Chapman et al., in which the highly collimated synchrotron source from X15A beamline of the National Synchrotron Light Source (NSLS) in Brookhaven National Laboratory was used, the obtained DEI images have shown details and characteristics not detected by conventional imaging [2–5]. In Chapman et al. DEI setup, the system employed Si(3 3 3) crystals for producing monochromatic and diffracted X-ray beams, which is refracted through a very small angular deflection of the order of micro-radian. This arrangement made it possible to obtain higher contrast images from the same object. However, the use of a synchrotron source necessitates having a DEI system close to a major synchrotron facility. A clinically approved DEI system, which may be installed in major hospitals, would need a new X-ray source that can provide a substitute for a synchrotron source. Other applications of high-resolution enhanced radiography may be extended to material science research and crystallography such as 3-D

*Corresponding author. Tel.: +1 919 645 8015.
E-mail address: Chkim4@unity.ncsu.edu (C.H. Kim).

0168-9002/$ - see front matter © 2006 Elsevier B.V. All rights reserved.
doi:10.1016/j.nima.2006.07.041

mapping of composite materials, grains in polycrystalline materials, distribution of elements in cells and imaging of sprays [6,7]. Additionally, there would be other potential industrial applications such as advanced radiography for cargo and parcel screening with enhanced resolution for active interrogation techniques.

The purpose of this study is to investigate the feasibility of developing a new compact size area X-ray source capable of producing photon fluxes of sufficient intensity and quality needed for diffraction-enhanced imaging without using a synchrotron source. This computational study is a first step from laboratory testing version towards developing a proto-type system as a clinically approved DEI system for medical radiology followed by scalability to other applications. The desirable features of an area X-ray generator compatible to a synchrotron source to satisfy DEI requirements are [10–12]:

- Peak electric power less than 200 kW, 3 A beam current at 60 kVp.
- High target flux ($\sim 10^{12}$ ph/mm^2/s) to be compatible to the synchrotron source target flux.
- Output X-ray beam collimated over a 100 cm^2 area.
- Reasonable operation time (5–10 s).
- Stationary target assembly and concentric or spiral filament configuration.

The major aspects of this study are the electrostatic analysis and electron trajectories and their distribution, the thermal analysis and target heat loading for appropriate operation time, and investigation of X-ray energies and X-ray flux at the extraction window of the system.

2. General considerations

The white beam from the X15A beamline at NSLS delivers a target flux of 1.4×10^{12} ph/s/mm^2/keV at 18 keV. After the beam went through Si[1 1 1] double crystal monochromator, the flux drops $\sim 10^7$ ph/s/mm^2/keV at 18 keV. Typical scanning time to acquire an image with such synchrotron beam is in the range of 4–200 s [11]. A conventional X-ray tube, operating with thermionic emission filaments, may be used to substitute for the X-ray source. However, conventional X-ray tubes have continuous spectra and low beam intensity as compared to synchrotron sources [8]. The Bremsstrahlung radiation from a conventional X-ray tube delivers unnecessary radiation dose to the patient, and is not useful for DEI applications. Moreover, the low beam intensity increases the scan time, which is estimated to be between 1000 and 10,000 s for a conventional source. In addition, a collimated area X-ray beam can provide area magnification for DEI applications. A conventional X-ray tube typically operates with a 0.3–0.4 mm focal spot [9]. For a clinically approved DEI mammography unit, the dimension of the beam in the sagittal direction will be 150 mm to get a full field of view.

Several concepts for a new X-ray source were proposed by a North Carolina State University research group in collaboration with a University of North Carolina Chapel Hill Radiology group and others, such as the shaped-target multi-filament concept, the high-current beam steering concept and the cold cathode field emission concept [10,11]. Of these, the shaped-target multi-filament concept has the most attractive features. In this concept, the source design is based on a tilted stationary molybdenum target with the target's surface shaped in a log-spiral. Filaments are arranged as an array of line filaments, with each filament assembly composed of the individual line filaments and corresponding focus cups. Total emission current of the filament array can be as high as 3 A, which will deliver a total power of 180 kW to the target at 60 kVp operation. The illumination area for this concept is 150×150 mm, however, a 50×50 mm prototype was proposed [12]. An evolution from this concept is the area X-ray source using concentric circular filaments and a stationary tilted oxygen-free copper target with a thin layer of molybdenum. This proposed target configuration would allow for better thermal management, as the target body is copper.

Increasing the accelerating potential produces higher X-ray intensity, which includes higher Bremsstrahlung in the X-ray spectrum. The higher Bremsstrahlung in the X-ray spectrum may also produce higher radiation dose to patient. The generated Bremsstrahlung radiation could be reduced or eliminated through the use of aluminum or beryllium filtering windows. Increasing the electron beam current, which depends on electron emission area from the filament, is another means by which the X-ray intensity could be increased. The typical X-ray tube uses a very small line filament, which acts as a point source not exceeding the area of the target. Concentric circular filaments increase the emission area over the standard spot-size filament source. The large electron emission area produces higher electron beam current, and higher electron flux, thus increasing the number of electrons illuminating the target surface. Both increasing accelerating potential and a larger electron emission area, result in increased heat loading of the X-ray target. The heat loading would exceed the cooling capacity of typical X-ray tubes, which usually use a rotating target to spread the heat loading over the rotating area, or an air-cooling system. Therefore, a concentric filament X-ray source operating at higher beam currents up to 3 A will necessitate the use of an active cooling system for heat removal.

For this study, the designed area X-ray generator is composed of a stationary target made of oxygen-free copper with a thin molybdenum layer, a filament assembly composed of three concentric circular filaments, an active cooling system for the target and the overall housing of the source assembly. The core of this research is to investigate the source electrostatics and generation of the electrons and their trajectories, target thermal loading and thermal management and X-ray generation. Electron trajectories and their distribution in the system are determined by the

geometry of the anode and cathode, and the form of electron acceleration. Analysis of electron trajectories and their distribution is conducted using SIMION 3D [13]. As accelerated electrons impact on the target most of their kinetic energy is converted to heat, raising the target temperature (which may exceed its melt temperature) and limits the operational time. For this purpose thermal calculations are performed using the coupled FEMLAB multi-physics and MATLAB codes. The quality and intensity of the produced X-rays are related to the target material and the electron accelerating potential, the Monte Carlo code MCNP 5 has been used for this analysis [14–16].

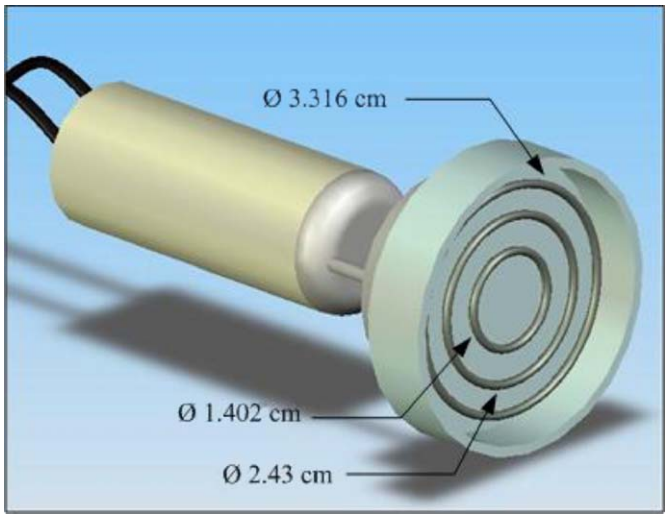

Fig. 1. Illustration of the filament assembly showing the three concentric filaments inside the filament cup.

Table 1
Parameters of the circular filaments

Filaments material: tungsten	Radius (cm)	Total length (cm)
Inner	0.701	4.404
Middle	1.215	7.634
Outer	1.658	10.417

3. Filament-target design

Three concentric circular filaments provide the required area magnification necessary for a DEI system. The total length of the filament array is about 22.5 cm, which is about 50 times longer than a filament in a conventional X-ray source. Fig. 1 shows an illustration of the filament assembly. The design parameters are shown in Table 1. The target is made of oxygen-free copper covered with a thin (<1.0 mm thick) molybdenum layer via sintering, however, other techniques such as plasma sputter deposition could be used to manufacture such targets. The molybdenum surface area is 6.157 cm^2. Fig. 2 shows the target geometry, and the target parameters are shown in Table 2 [17].

4. Simulation considerations

4.1. Electrostatics and particle trajectories simulation

Electron trajectories and particle distributions are simulated using the SIMION code assuming a 22.5° take off angle. The simulation allows for varying the electric field configuration, and a floating or non-floating filament cup base (backing plate). The power supply for the filaments is separate from the high-voltage supply, which supplies the accelerating potential between the cathode and the target. The filament base cup is set at negative potential and the X-ray target is grounded. The filament supply is floating, however, if desired one of the filament leads may be connected to the focusing cup such that they together work as a cathode, or the filament may have a high-voltage connection different from the cup potential and its supply current float on top of the high voltage. Fig. 3 illustrates

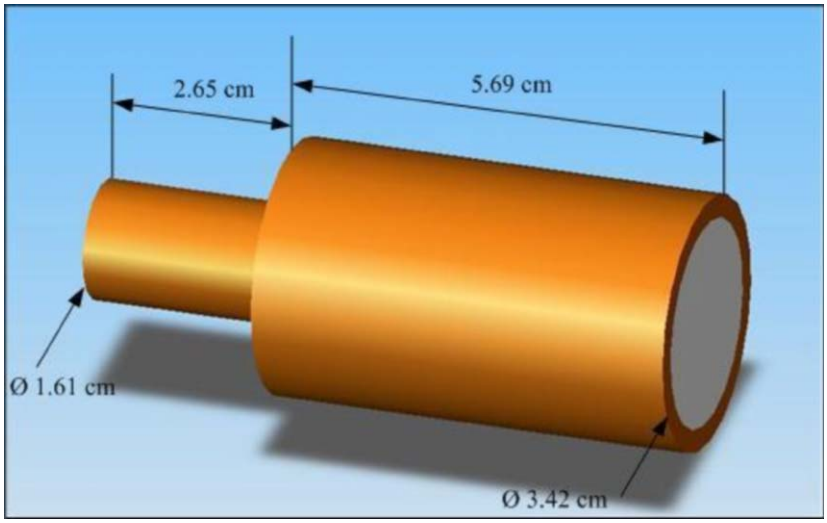

Fig. 2. Geometry of the stationary target showing the copper body and molybdenum layer.

Table 2
Stationary target parameters and thermal properties [17]

	Radius (cm)	Length (cm)	Thermal conductivity (W/cm K)	Melting point (K)
Cu Body	1.71	5.69	1.48	1357
Mo layer	1.40	<0.1	4.01	2896

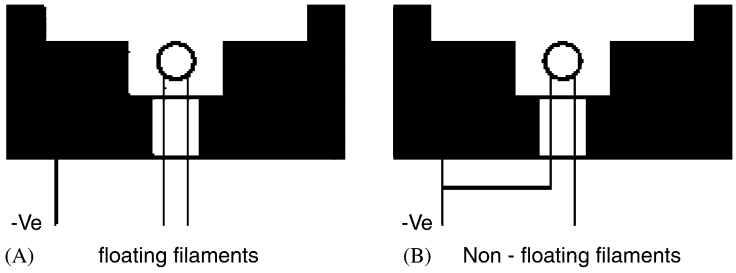

Fig. 3. Floating and non-floating filament configurations.

the configuration of the concentric filament and focusing cup assembly for the floating and non-floating (biased) options.

4.2. Thermal analysis simulation

The main heat transfer mechanism in the thermal simulation is conduction, although the actual target would emit some heat via radiation as the entire source is under vacuum. In this simulation the target front receives the inward heat flux from the electron beam, the back of the target is maintained at liquid nitrogen temperature, and the target body is assumed thermally insulated with vacuum boundaries. The properties of the target material and its geometrical shape are important factors in the thermal conduction analysis. The target is a thin (<1 mm thick) layer of molybdenum on top of an oxygen-free cylindrical copper block. As molybdenum's melting point (2623 °C) is much greater than that of copper (1085 °C), the copper block will reach its melting point before the molybdenum if the heat loading is excessive. As a result, in these simulations the thermal resistance of the thin molybdenum layer was ignored. To perform the thermal analysis, electron beam energy and distribution at the surface of the target are used as inputs to the 3-D finite element code FEMLAB. The option of the filament connected to the backing plate acting as the cathode at −60 kV was chosen as the test case because it shows the least particle loss and the best focusing of the beam on the target. Four beam current test cases were considered, 3, 30, 300 mA, and 3 A. In all four cases, the spatial distribution of the target's temperature is obtained as a function of time, with the limiting factor set to the time-to-melt of the copper surface facing the incoming electron beam.

4.3. Characteristic X-ray simulation

The MCNP 5 Monte Carlo code has been used to calculate X-ray production and radiation dose at the extraction window. The K-shell characteristic X-rays for a molybdenum target are the $K_{\alpha 1}$ (17.48 keV), $K_{\alpha 2}$ (17.37 keV) and $K_{\beta 1}$ (19.61 keV). The X-ray intensity at the extraction window depends on the window material and its thickness. Two window materials, aluminum and beryllium, are used in this simulation with three different window thicknesses of 0.1, 0.05 and 0.01 mm for each. The selection of these two window materials and their respective thickness are intended to optimize the maximum flux of the $K_{\alpha 1}$ and $K_{\alpha 2}$ lines, and possibly the $K_{\beta 1}$ line too. It is also important in determining the optimal window design that could support such a thin large area window subject to the high vacuum condition without breaking or failure.

5. Simulation results

5.1. Electron distribution on the target

Simulation of the first option, in which the filament acts as a cathode and is biased by negative 12 Vp while the backing plate (filament cup) is at negative 60 kVp, results in an electron distribution on the target, which is almost uniform as shown in Fig. 4. However, the diverging electric field results in electron trajectories, which miss the target surface. Although target illumination is uniform and reasonable for the production of an area beam, the expected X-ray intensity is low. Fig. 5 shows the electron deposition distribution on the target surface. This option could be used for generating an area X-ray beam by lining the interior of the housing with lead to overcome shielding problems emanating from diverging electrons, and by increasing beam current to increase X-ray intensity. Increasing the beam current could be accomplished by

increased thermionic emission from the filament, which may lead to either shorter filament lifetime or filament failure at high temperatures; or by increasing the acceleration potential at same beam current, which makes the entire system impractical.

In the simulation of the second option, in which the filament acts as the cathode at −60 kVp and is connected to the focusing cup, the loss of electrons is minimal, as shown in Fig. 6, and their distribution on the target is nearly uniform except for a peak at the center of the target, as shown in Fig. 7. The hotspot could be filtered out via X-ray optics or by further optimization in this configuration.

5.2. Target thermal loading

Because of the assumption that the back of the target is maintained at liquid nitrogen temperature (liquid nitrogen contacted target), and the target body is thermally insulated, the initial target temperature was set for all cases to 77 K assuming the target is already cooled prior to operation. The heat flux on the surface of the target is obtained from the SIMION simulation electron distribution and transient thermal analysis was performed using FEMLAB. The maximum temperature of the target's surface reaches 270 K in 300 s for a 300 mA beam current, which indicates that the operation with such beam current is almost near steady state. For lower beam currents of 3 and 30 mA, the maximum temperatures are 77 and 90 K in 100 s, respectively (almost maintained at liquid nitrogen temperature). Therefore, in the case of 300 mA, with 270 K reached in 300 s the system could serve enough operation time without heat loading concerns, however, to reach sufficient target flux, a 3 A beam current would be required. In the 3 A beam current case, the target temperature reaches 1357 K in 70 s, which is the melting point of copper. Thus, the liquid nitrogen contacted target configuration

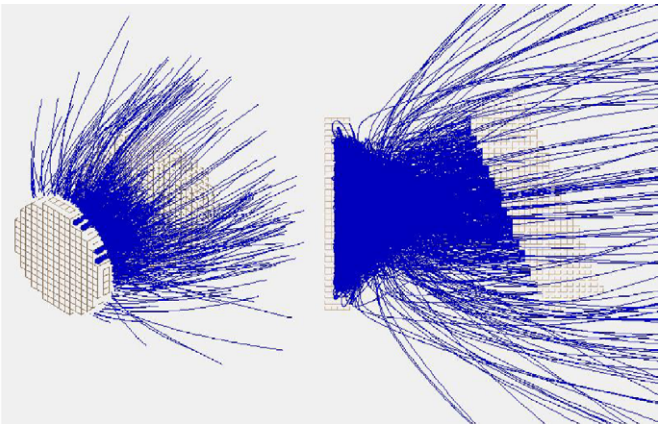

Fig. 4. Electron trajectories with −60 kVp focusing cup and filaments at −12 Vp.

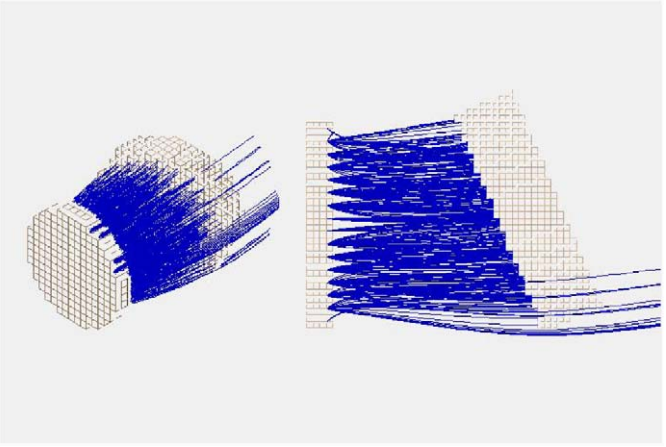

Fig. 6. Electron trajectories with −60 kVp focusing cup and filaments.

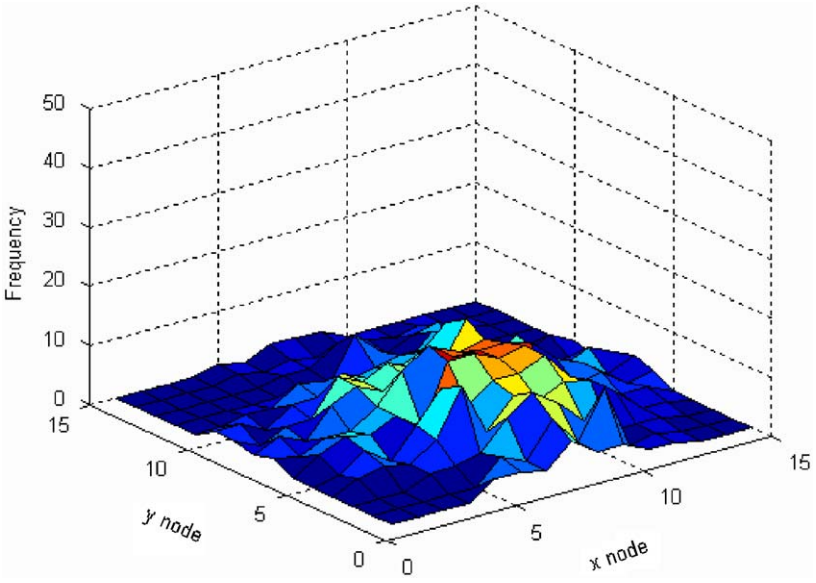

Fig. 5. Electron deposition distributions with −60 kVp focusing cup and filaments at −12 Vp.

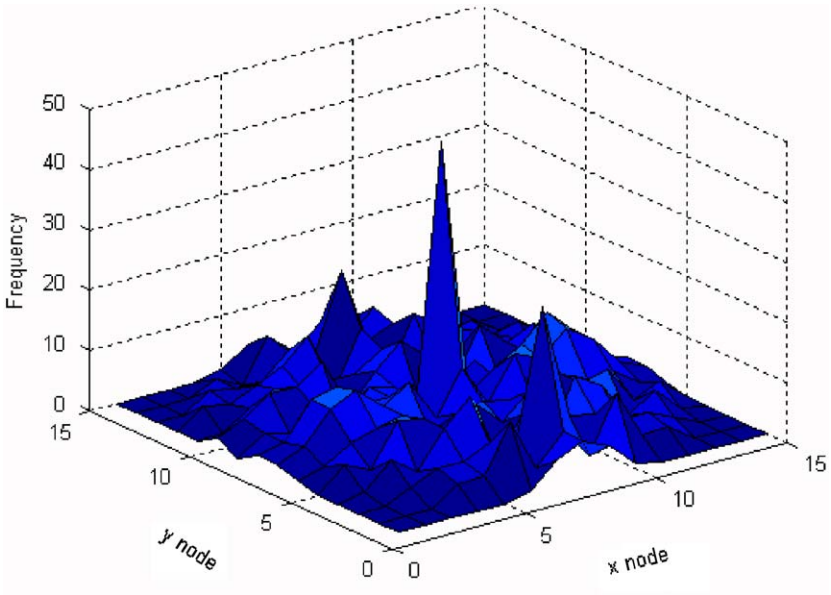

Fig. 7. Electron deposition distributions with −60 kVp focusing cup and filaments.

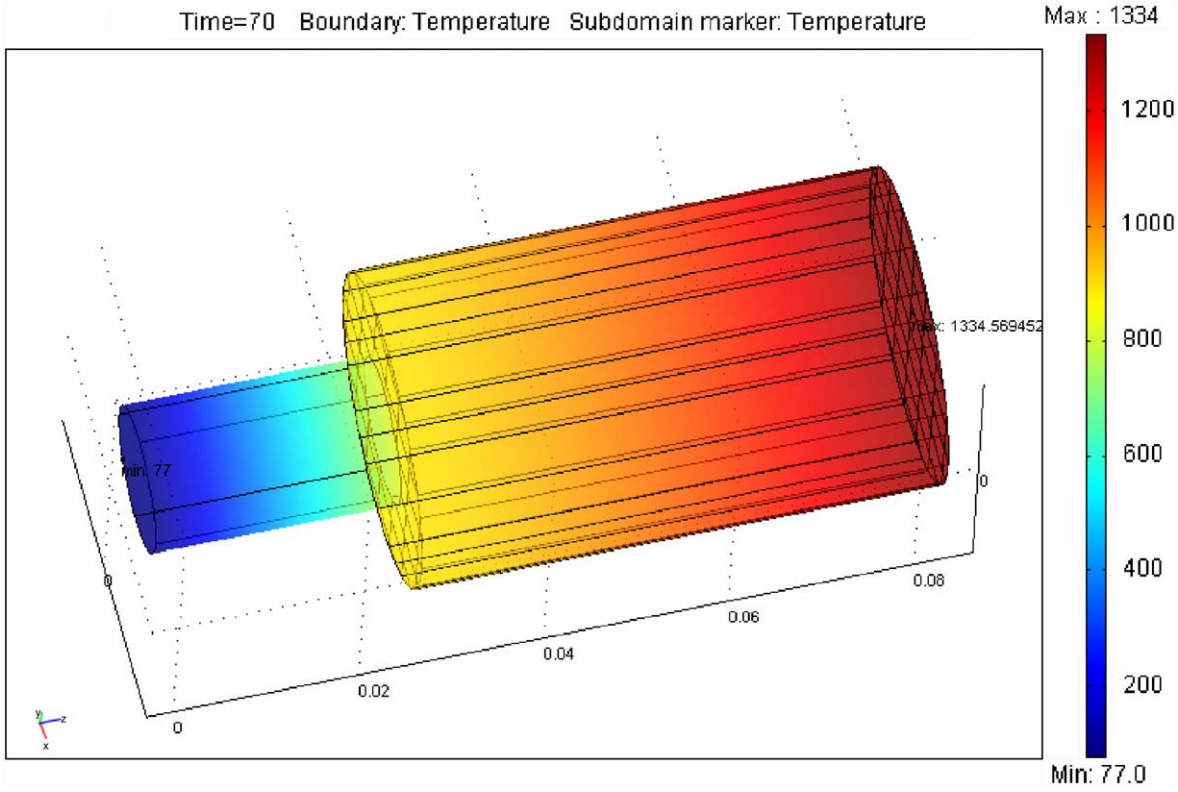

Fig. 8. Target temperature distributions at 70 s, target at −60 kVp with 3 A beam current.

does not provide sufficient operation time. Fig. 8 shows the temperature distribution for the 3 A, −60 kVp in 70 s operation.

In order to provide better thermal management, invaded target configuration was investigated, in which liquid nitrogen is introduced into the target body and closer to the target front. Fig. 9 shows the invaded target temperature distribution for 3 A, −60 kVp in 15 s operation.

Simulation results of the invaded target configuration at 3 A beam current show that the maximum target surface temperature reaches 325 K in 10 s, and remains unchanged

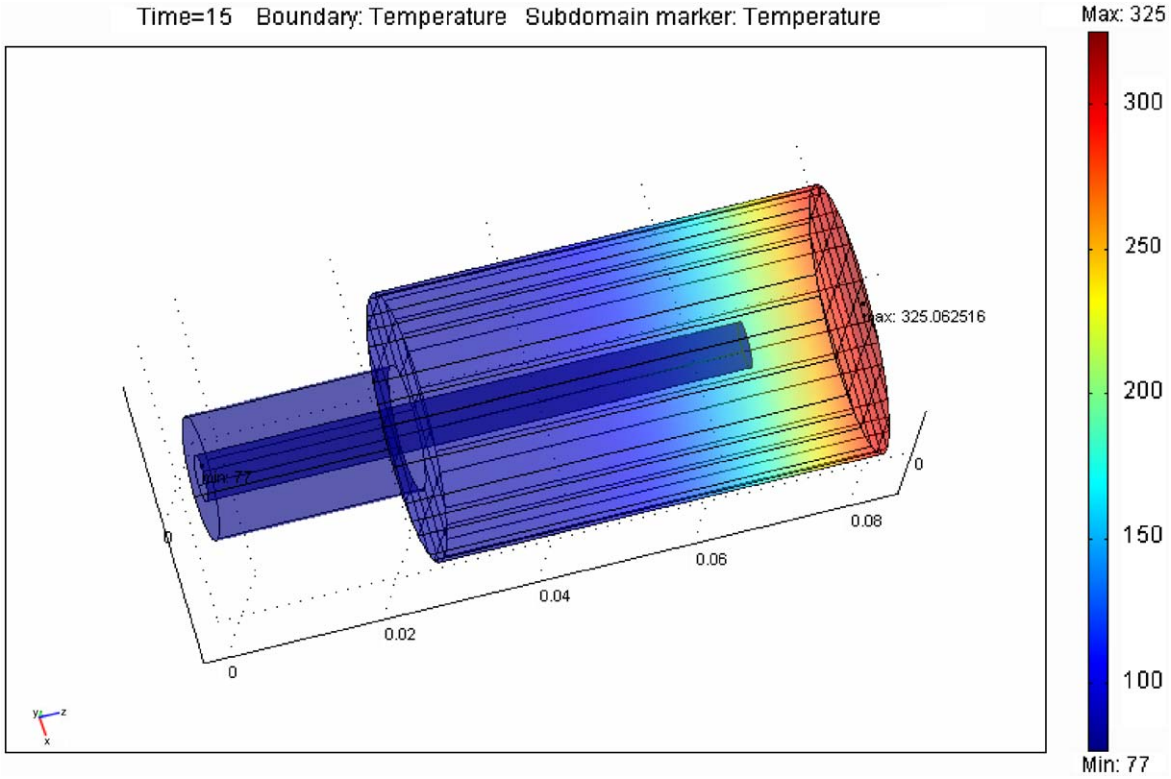

Fig. 9. Target temperature distributions at 15 s, target invaded by liquid nitrogen, at −60 kVp with 3 A beam current.

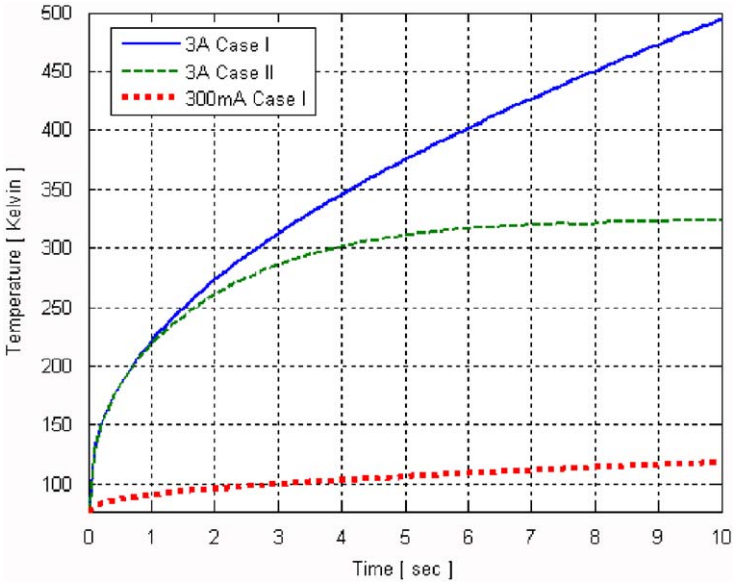

Fig. 10. Maximum target surface temperatures up to 10 s for −60 kVp at 300 mA and 3 A beam currents with contacting cold finger (Case I), and 3 A with liquid nitrogen invaded target (Case II).

thereafter. Fig. 10 shows the maximum target surface temperature as a function of time for 10 s (for the details of initial temperature rise) for 300 mA and 3 A (contacted target, Case I); and for 3 A beam current (invaded target, Case II), while Fig. 11 shows the temperature for both cases up to 100 s.

5.3. Output X-ray flux

The MCNP simulation results are shown in Fig. 12 for aluminum and beryllium, for window thicknesses of 0.01 and 0.05 mm. The normalized characteristic $K_{\alpha 1}$, $K_{\alpha 2}$ and $K_{\beta 1}$ X-ray intensities (particles/mm^2 per total number of

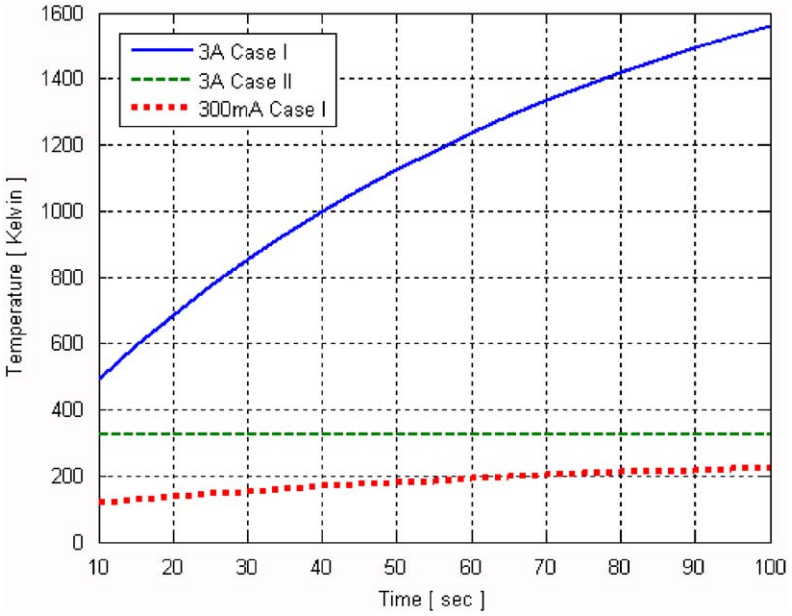

Fig. 11. Maximum target surface temperatures up to 100 s for −60 kVp at 300 mA and 3 A beam currents with contacting cold finger (Case I), and 3 A with liquid nitrogen invaded target (Case II).

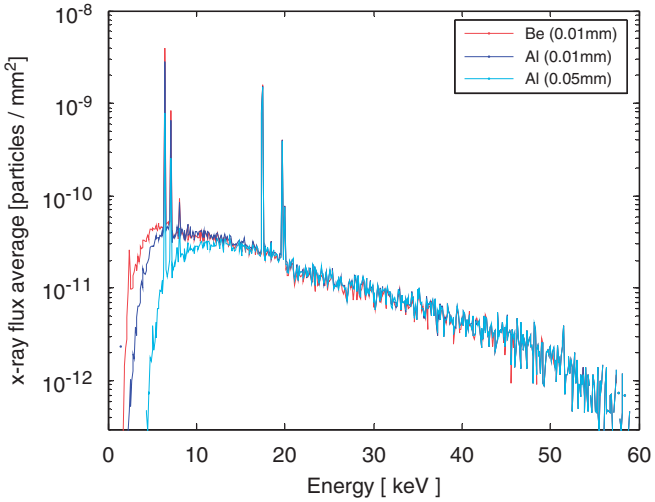

Fig. 12. X-ray spectra with Be and Al window, −60 kVp acceleration.

source particles) are shown in Table 3 for each window thickness. For a given beam current, multiplying the normalized intensity by the total number of the electrons hitting the target (source particles) yields the X-ray intensity for this specific beam current. Aluminum window results show increased intensity with decreased window thickness, while there is no significant change for beryllium windows. However, aluminum windows are more efficient at removing lower energy Bremsstrahlung, which only contributes to the radiation dose. This means that achieving higher X-ray intensity using aluminum windows would require a very thin window, which imposes structural difficulty for a large window under high vacuum. For beryllium, it appears that the window thickness is not a factor and a thicker window might be used. This may be helpful in the engineering design of the window with stronger structure integrity.

The normalized X-ray intensities are obtained from the probability calculated by MCNP multiplied by the total number of electrons per second to obtain the photon flux ($ph/mm^2/s$) for the line of interest that corresponds to the beam current. For a beam current of 3 A, the $K_{\alpha 1}$ X-ray flux for 0.01 mm aluminum window is 2.92×10^{10} $ph/mm^2/s$. For a 0.1 mm beryllium window the computed flux is 2.96×10^{10} $ph/mm^2/s$. Although such window thickness appears to be thin, however techniques of sputter deposition of such thickness are achievable on vacuum glass viewing ports. These X-ray fluxes are less than the synchrotron radiation flux, $\sim 10^{12}$ $ph/mm^2/s$, implying that for a scaled up device area magnification would be necessary to achieve higher flux. The model used in this study is for the molybdenum target area of 6.157 cm^2 and beam current of 3 A. Scaled up device with target surface area of 100 cm^2 provides a factor of 16.242 area magnification. Thus, an overall increase in photon flux would be a factor of 16.242 greater and a flux of 4.808×10^{11} $ph/mm^2/s$ could be achieved, which is comparable to a synchrotron flux of $\sim 10^{12}$ $ph/mm^2/s$.

6. Conclusions

Computational studies of a prototype concentric filament area X-ray source with a tilted stationary target made of molybdenum layer sintered on copper have shown the capability to produce target flux compatible to that of a synchrotron source target flux.

Electron trajectories and their distribution on the target were computed for two different configurations. The backing plate at −60 kVp and the filament biased by

Table 3
MCNP results with Al and Be window

Material	Thickness (mm)	$K_{\alpha 1}$ (particles/mm^2)	$K_{\alpha 2}$ (particles/mm^2)	$K_{\beta 1}$ (particles/mm^2)
Al	0.01	1.56E−09	8.27E−10	3.99E−10
	0.05	1.49E−09	7.83E−10	3.87E−10
	0.1	1.39E−09	7.32E−10	3.66E−10
Be	0.01	1.58E−09	8.35E−10	4.03E−10
	0.05	1.58E−09	8.34E−10	4.03E−10
	0.1	1.58E−09	8.34E−10	4.02E−10

−12 Vp produces a uniform distribution, however, there was a loss of electron population and many electrons miss the target as a result of the diverging electric field. With both the filament and backing plate at −60 kVp the electrons are better focused on the target, which results in less background radiation. Thermal management was investigated with four beam currents, 3, 30, 300 mA, and 3 A. The maximum target surface temperature using a contact liquid nitrogen cold finger with a 3 A beam current exceeded the melting point of copper (1357 K) in 70 s. Using invaded target configuration at 3 A beam current, with liquid nitrogen circulating inside the target, showed that the maximum target surface temperature reaches 325 K in 10 s, and remains unchanged thereafter. The characteristic X-rays $K_{\alpha 1}$, $K_{\alpha 2}$ and $K_{\beta 1}$ of molybdenum target have been investigated for aluminum and beryllium window materials. Simulation results have shown that reduction of the Bremsstrahlung is better with aluminum window over beryllium. The $K_{\alpha 1}$ X-ray flux for a beam current of 3 A with 0.01 mm aluminum window is 2.92×10^{10} ph/mm^2/s, which is two orders of magnitude less than synchrotron source, however, area magnification to 100 cm^2 for a scaled up industrial system could provide the target flux required for DEI applications. An industrial scale device operating at 3 A beam current and a molybdenum target area of 100 cm^2 provides a target flux of 4.808×10^{11} ph/mm^2/s, which is compatible to a synchrotron source target flux. The use of a beryllium window would allow for higher flux at lower beam currents, with the advantage of having a thicker window over a thin aluminum one to sustain high vacuum requirements, however, plasma sputter deposition techniques could be used to deposit thin layer of beryllium on high vacuum viewing windows.

References

[1] F. Shtern, Radiology 183 (1992) 629.
[2] D. Chapman, W. Thomlinson, F. Arfelli, et al., Rev. Sci. Instrum. 67 (9) (1996) CD-ROM.
[3] D. Chapman, W. Thomlinson, R.E. Johnston, et al., Phys. Med. Biol. 42 (1997) 2015.
[4] E.D. Pisano, R.E. Johnston, D. Chapman, J. Geradts, M.V. Iacocca, C.A. Livasy, D.B. Washburn, D.E. Sayers, Z. Zhong, M.Z. Kiss, W.C. Thomlinson, Radiology 414 (3) (2000) 895.
[5] Z. Zhong, W. Thomlinson, D. Chapman, D. Sayers, Nucl. Instr. and Meth. A 447 (2000) 556.
[6] J.D. Budai, W. Yang, N. Tamura, J.-S. Chung, J.Z. Tischler, B.C. Larson, G.E. Ice, C. Park, D.P. Norton, Nat. Mater. 2 (487) (2003).
[7] A.G. MacPhee, M.W. Tate, C.F. Powell, Y. Yue, M.J. Renzi, A. Ercan, S. Narayanan, E. Fontes, J. Walther, J. Schaller, S.M. Gruner, J. Wang, Science 295 (1261) (2002).
[8] E. Abbramyan, Industrial Electron Accelerators and Applications, Hemisphere Publishing Corp., New York, 1988.
[9] J.T. Bushberg, et al., The Essential Physics of Medical Imaging, second ed., Lippincott Williams & Wilkins, Baltimore, MD, 2002.
[10] C.H. Kim, A study of an areas X-ray source for diffraction enhanced imaging for clinical and industrial application, M.S. Thesis, NC State University, August 2004.
[11] D. Chapman, Private Communication, 2001, 2002.
[12] E. Pisano, E. Johnson, D. Chapman, Z. Zhong, D. Sayers, K. Verghese, J.M. Doster, M.A. Bourham, M. Yaffee, Clinical diffraction enhanced mammography unit, NCSU and UNC-CH Invention Disclosure, NCSU File Number 01-59, July 2000.
[13] D.A. Dahl, Idaho National Laboratory, SIMION 3D version 7.0 User's Manual, 2000.
[14] J.A. Halbleib, The Integrated TIGER System in Monte Carlo Transport of Electrons and Photons, Plenum Press, New York, 1988.
[15] J.A. Halbleib, et al., The integrated TIGER series of Coupled Electron/Photon Monte Carlo Transport Codes, Sandia National Lab., Albuquerque, NM, SAND91-1634, 1991.
[16] MCNP—A General Monte Carlo N-Particle Transport Code—Version 5, ORNL/RSICC, April 2003.
[17] CRC Handbook of Chemistry and Physics, 84th ed., CRC Press LLC, 2003–2004.